ORIGINAL RESEARCH

NF-κB Mediates Mesenchymal Transition, Remodeling, and Pulmonary Fibrosis in Response to Chronic Inflammation by Viral RNA Patterns

Bing Tian[1,2], Igor Patrikeev[3], Lorenzo Ochoa[3], Gracie Vargas[3], KarryAnne K. Belanger[1,4], Julia Litvinov[1,5], Istvan Boldogh[2,5,6], Bill T. Ameredes[1,2,6], Massoud Motamedi[3], and Allan R. Brasier[1,2,6]

Departments of [1]Internal Medicine, [2]Sealy Center for Molecular Medicine, [3]Center for Biomedical Engineering [6]Institute for Translational Sciences, [4]Department of Biochemistry and Molecular Biology, and [5]Department of Microbiology and Immunology, University of Texas Medical Branch, Galveston, Texas

Abstract

Airway remodeling is resultant of a complex multicellular response associated with a progressive decline of pulmonary function in patients with chronic airway disease. Here, repeated infections with respiratory viruses are linked with airway remodeling through largely unknown mechanisms. Although acute activation of the Toll-like receptor (TLR) 3 pathway by extracellular polyinosinic:polycytidylic acid (poly[I:C]) induces innate signaling through the NF-κB transcription factor in normal human small airway epithelial cells, prolonged (repetitive or tonic) poly(I:C) stimulation produces chronic stress fiber formation, mesenchymal transition, and activation of a fibrotic program. Chronic poly(I:C) stimulation enhanced the expression of core mesenchymal regulators Snail family zinc finger 1, zinc finger E-box binding homeobox, mesenchymal intermediate filaments (vimentin), and extracellular matrix proteins (fibronectin-1), and collagen 1A. This mesenchymal transition was prevented by silencing expression of NF-κB/RelA or administration of a small-molecule inhibitor of the IκB kinase, BMS345541. Acute poly(I:C) exposure *in vivo* induced profound neutrophilic airway inflammation. When administered repetitively, poly(I:C) resulted in enhanced fibrosis observed by lung micro–computed tomography, second harmonic generation microscopy of optically cleared lung tissue, and by immunohistochemistry. Epithelial flattening, expansion of the epithelial mesenchymal trophic unit, and enhanced Snail family zinc finger 1 and fibronectin 1 expression in airway epithelium were also observed. Repetitive poly(I:C)-induced airway remodeling, fibrosis, and epithelial–mesenchymal transition was inhibited by BMS345541 administration. Based on this novel model of viral inflammation–induced remodeling, we conclude that NF-κB is a major controller of epithelial–mesenchymal transition and pulmonary fibrosis, a finding that has potentially important relevance to airway remodeling produced by repetitive viral infections.

Keywords: airway reprogramming; polyinosinic:polycytidylic acid; Toll-like receptor 3; epithelial–mesenchymal transition; tissue clearing

Asthma is a chronic inflammatory disorder of the airways manifested by reversible episodic bronchoconstriction, triggered by environmental and infectious stimuli. Over 300 million adults and children suffer from this disease, making this an important public health problem (1). Asthma represents a constellation of phenotypes, due to complex gene–environmental interactions. Although bronchoconstriction is typically reversible, a subset of subjects with asthma develop progressive decline in pulmonary function with age, a process thought to be due to irreversible airway remodeling and fibrosis (2). Similarly,

(Received in original form August 15, 2016; accepted in final form November 11, 2016)

This work was supported, in part, by National Institutes of Health National Institute of Allergy and Infectious Diseases grants AI062885 (A.R.B.), UL1TR001439 (A.R.B.), National Institute of Environmental Health Sciences grants T32ES007254 (B.T.A.) and ES006676 (A.R.B. and B.T.A.), National Science Foundation grant DMS-1361411/DMS-1361318 (A.R.B.), the Sealy Center for Molecular Medicine, the Sealy Center for Environmental Health and Medicine, and the Brown Foundation. Core laboratory support was provided by the University of Texas Medical Branch Immunohistochemistry Core and the Optical Imaging Cores.

Author Contributions: Conception and design—B.T., G.V., B.T.A., M.M., and A.R.B.; analysis and interpretation—B.T., I.P., L.O., G.V., A.R.B., I.B., M.M., and A.R.B.; writing—B.T., G.V., K.K.B., J.L., B.T.A., M.M., and A.R.B.

Correspondence and requests for reprints should be addressed to Allan R. Brasier, M.D., MRB 8.126, University of Texas Medical Branch, 301 University Boulevard, Galveston, TX 77555-1060. E-mail: arbrasie@utmb.edu

Am J Respir Cell Mol Biol Vol 56, Iss 4, pp 506–520, Apr 2017

Originally Published in Press as DOI: 10.1165/rcmb.2016-0259OC on December 2, 2016
Internet address: www.atsjournals.org

Clinical Relevance

Airway remodeling causes a progressive decline of pulmonary function in patients with obstructive lung disease. Airway remodeling is caused by respiratory virus infections through largely unknown mechanisms. Our study demonstrates that repetitive activation of viral response pathways produces inflammation, mesenchymal transition of epithelial surface, and fibrosis. Our studies implicate the NF-κB pathway in the mediation of this process, identifying NF-κB as a target for reducing inflammation-mediated remodeling.

airway remodeling is linked to progressive declines in airway function seen in patients with chronic airway disease, including chronic obstructive pulmonary disease and cystic fibrosis (3, 4).

Airway remodeling is a constellation of structural changes that includes disruption of the epithelial barrier function, subepithelial fibrosis, myofibroblast hyperplasia, and smooth muscle hypertrophy (2, 5). Although airway remodeling is a complex, multicellular phenomenon triggered by environmental, age-related, and genetic factors (6), we now know that chronic epithelial injury can play a fundamental role. In this case, disruption of the epithelial barrier induces secretion of epithelial growth factors (transforming growth factor [TGF]-β, epidermal growth factor) and cytokines (periostin, IL-17, IL-11) that initially promote re-epithelialization and fibrosis, initial stages important in mucosal repair (7). Although this process initially plays a homeostatic function in mucosal injury, its prolonged action is associated with organ fibrosis and progressive decline in lung functions in a subset of patients who suffer its unremitting effects (8).

The signal transduction pathway triggered by TGF-β through its type II receptor (TGF-βRII) is now well understood and known to be an important part of the epithelium-associated remodeling process. TGF-βRII activates epithelial programs through interacting Smad-dependent and Smad-independent pathways (9); these pathways converge on activating the transcriptional corepressor, Snail family zinc finger (SNAI) 1. SNAI1, in turn, directly binds to regulatory promoter regions of E-cadherin (CDH1) and zona occludens-1, leading to their repression and subsequent cellular loss of apical–basal polarity (10). Separately, SNAI1 up-regulation induces zinc finger E-box binding homeobox (ZEB) 1, a separate epithelial–mesenchymal transition (EMT) core regulator, to produce a multistep dedifferentiation program referred to as type II EMT (11). In this manner, TGF-β induces epithelial cells to express mesenchymal smooth muscle cell actin and intermediate filament vimentin (VIM), enhancing motility, and secrete collagen (COL), fibronectin (FN), and matrix metalloproteinases, promoting extracellular matrix deposition (12). Consequently, this response promotes airway remodeling with expansion of the smooth muscle cell layer, repair of the epithelial surface, and, ultimately, interstitial fibrosis (11, 13). Clinically, features of mesenchymal transition have been observed in subsets of subjects with severe asthma and chronic obstructive pulmonary disease (COPD) with remodeling; however, the role of mesenchymal transition has yet to be fully established (7, 9, 14).

Epidemiological studies have shown that recurrent viral airway infections are the most common cause of exacerbations in obstructive lung diseases (2, 15–18); these infections lead to an accelerated decline in lung function through poorly defined mechanisms (19). The epithelium plays a major role in the response to mucosal viruses by pattern-recognition receptor–induced innate response, producing inflammation and antiviral responses (20). Recently, we used unbiased gene expression profiling studies to identify a central role of the NF-κB transcription factor in the TGF-β–induced type II EMT gene program through its ability to directly trigger expression of SNA1, FN1, and the IL-6 growth factor (21). These studies indicated a direct, molecular link between innate inflammation and airway fibrosis (13, 21).

Reasoning that NF-κB activation may be sufficient to activate the EMT program, we examined the role of NF-κB activation by chronic activation of the innate response *in vitro* and *in vivo*. We describe here that chronic stimulation of primary human airway epithelial cells with the double-stranded RNA mimic and Toll-like receptor (TLR) 3 agonist (22), polyinosinic:polycytidylic acid (poly[I:C]), induced a time-dependent expression of NF-κB, EMT regulators, and the fibrotic program. Repetitive intranasal poly(I:C) administration *in vivo* induced morphological changes of airway epithelial cells in the conductive airways, with evidence of enhanced fibrosis in medium and small airways. These changes were associated with proximal and small-airway epithelial expression of SNA1, FN1, and COL1A, indicating mesenchymal transition. The remodeling and fibrotic program was completely inhibited by administration of the highly selective small-molecule IκB kinase (IKK) inhibitor. These data provide a new model for the study of innate inflammation–associated airway fibrosis and mechanistic insights into the role of the IKK–NF-κB pathway in epithelial cell state changes.

Materials and Methods

Detailed Materials and Methods are available in the online supplement.

Results

Persistent TLR3 Pathway Activation Induces Mesenchymal Transition of Airway Epithelial Cells

In this study, we investigated the effects of poly(I:C) on EMT in telomerase-immortalized primary cultures of human small-airway epithelial cells (hSAECs) (13, 21, 23, 24). We selected hSAECs for our *in vitro* studies, because they maintain a stable epithelial morphology, express differentiated airway epithelial cytokeratin isoforms after hundreds of population doublings, form pseudostratified columnar epithelium in air–liquid interfaces, and support the replication of mucosal-restricted viruses (25–27). Unbiased whole-genome studies show that these cells maintain gene expression patterns of primary cells (23). Similarly, proteomics profiling indicated that these cells secrete cytokeratin patterns and viral-induced inflammatory protein patterns that faithfully reproduce explants of primary human small-airway cells (24). Moreover, these cells have a functional NF-κB signaling pathway linked to TGF-β–induced mesenchymal transition (21),

and therefore have many characteristics representative of primary lower-airway epithelial cells.

We observed that extracellular poly(I:C) stimulation rapidly activated NF-κB/RelA nuclear translocation in confocal immunofluorescence (IF) assays (Figure 1A). By contrast, chronic poly(I:C) stimulation induced hSAECs to assume an elongated shape with markedly reorganized stress fibers extending throughout the cytoplasm over a wide concentration range (1–50 μg/ml) (Figure 1B). This morphological change of enhanced front–rear polarity and actin rearrangement are characteristic morphological changes of epithelial dedifferentiation produced by the TGF-β–induced EMT program (Figure 1B) (13, 21).

IF microscopy was used to further evaluate this cell state change. In untreated hSAECs, CDH1 is detectable in the periphery of the cytoplasm/cell junctions and in cytoplasmic aggregates, whereas VIM staining is faintly detectable in the cytoplasm (Figure 1C). There were low levels of SNAI1 expression in punctate foci within the nucleus, and RelA was located within the cytoplasm, characteristic of its inactive state. By contrast, in poly(I:C)-stimulated cells, CDH1 expression was no longer detectable, and intense VIM staining was seen in organized cytoplasmic bundles (Figure 1C). SNAI1 staining was increased throughout the cell, particularly in the nucleus. These staining patterns are similar to those of TGF-β–induced EMT (Figure 1C). Importantly, in RelA, nuclear translocation is observed in response to both EMT activating stimuli. The pathways controlling NF-κB activation in response to TGF-β have been partially investigated (21, 28). These data indicate that chronic poly(I:C) stimulation induces typical cellular features of EMT.

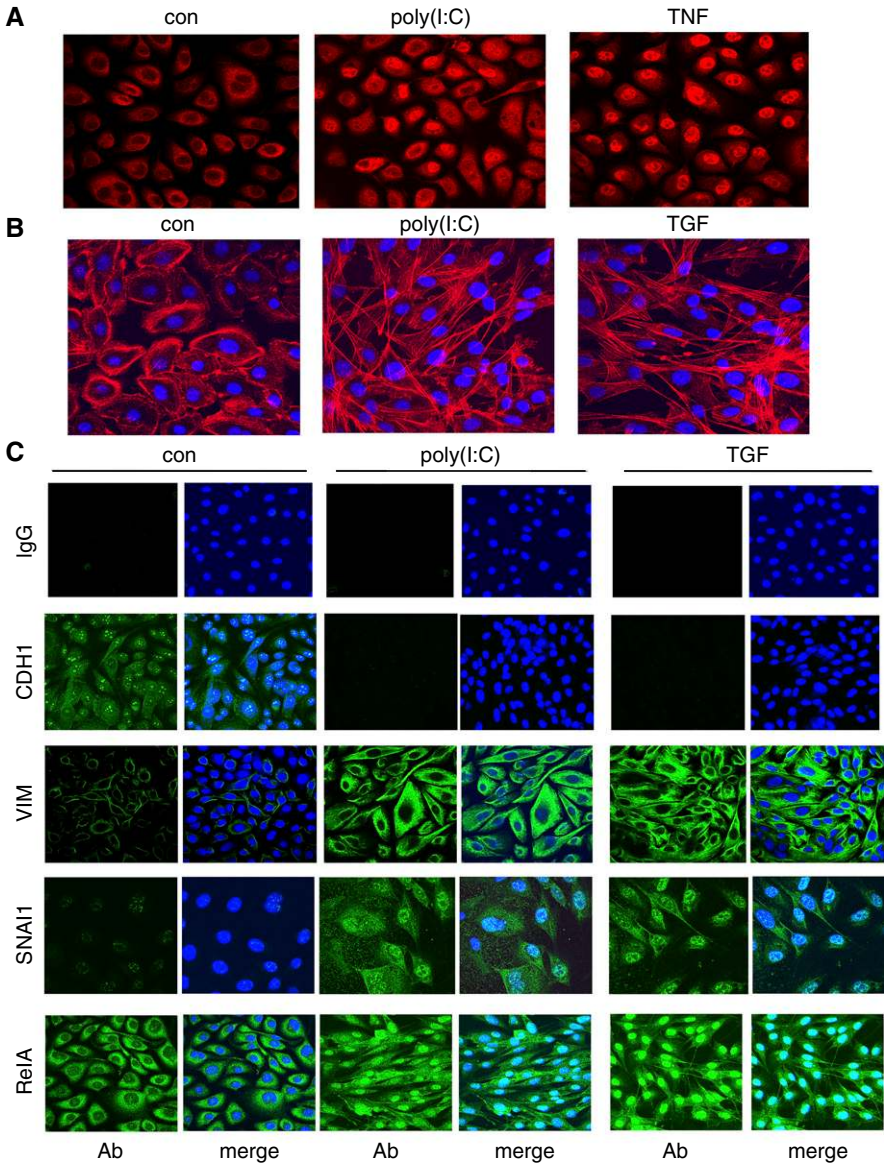

Figure 1. Polyinosinic:polycytidylic acid (poly[I:C]) induces NF-κB activation, actin stress fiber formation, and mesenchymal transition. (*A*) Poly(I:C) induces NF-κB/RelA nuclear translocation. Primary human small airway epithelial cells (hSAECs) were mock stimulated with vehicle (con), poly(I:C) (10 μg/ml, 2 h), or TNF (20 ng/ml, 1 h), the latter as a positive control. Cells were fixed, permeabilized, and stained with anti-RelA antibody (Ab), then stained with AlexaFluor568-conjugated goat anti-rabbit IgG and counterstained with 4′,6-diamidino-2-phenylindole (DAPI). Shown are confocal immunofluorescence micrographs. *Note* the strong translocation of RelA into the nucleus in both the poly(I:C)- and TNF-stimulated cells. (*B*) Poly(I:C) induces stress fiber formation. Primary hSAECs were incubated in the absence or presence of poly(I:C) (10 μg/ml) or transforming growth factor (TGF)-β (10 ng/ml) for 15 days. Cells were fixed, stained with Alexa568-conjugated phalloidin (*red*), and examined by confocal microscopy. (*C*) Poly(I:C) induces mesenchymal transition. Primary hSAECs were stimulated with poly(I:C) or TGF-β, as described previously here. Cells were fixed, permeabilized, and incubated with IgG or anti–E-cadherin (CDH1), vimentin (VIM), Snail family zinc finger (SNAI)-1, or RelA Abs, then stained with AlexaFluor488-conjugated goat anti-rabbit IgG (shown in *green*), counterstained with DAPI (*blue*), and imaged via fluorescence microscopy.

NF-κB/RelA Is Required for Poly(I:C)-Induced Mesenchymal Transition

Both acute and tonic poly(I:C)-stimulation induced RelA nuclear translocation (Figures 1A and 1C). To identify whether the EMT gene program was activated, we observed that repetitive, short-term poly(I:C) stimulation (for 1 h daily) would down-regulate the epithelial marker, CDH1, and/or up-regulate the mesenchymal markers, VIM and SNAI1 (Figure 2A). Because both repetitive daily stimulation and tonic stimulation with poly(I:C) produced similar effects on the mesenchymal transition, for convenience, in subsequent experiments we stimulated hSAECs tonically with poly(I:C).

To determine whether RelA was functionally required for the mesenchymal transition, we examined the effect of NF-κB/RelA silencing using doxycycline

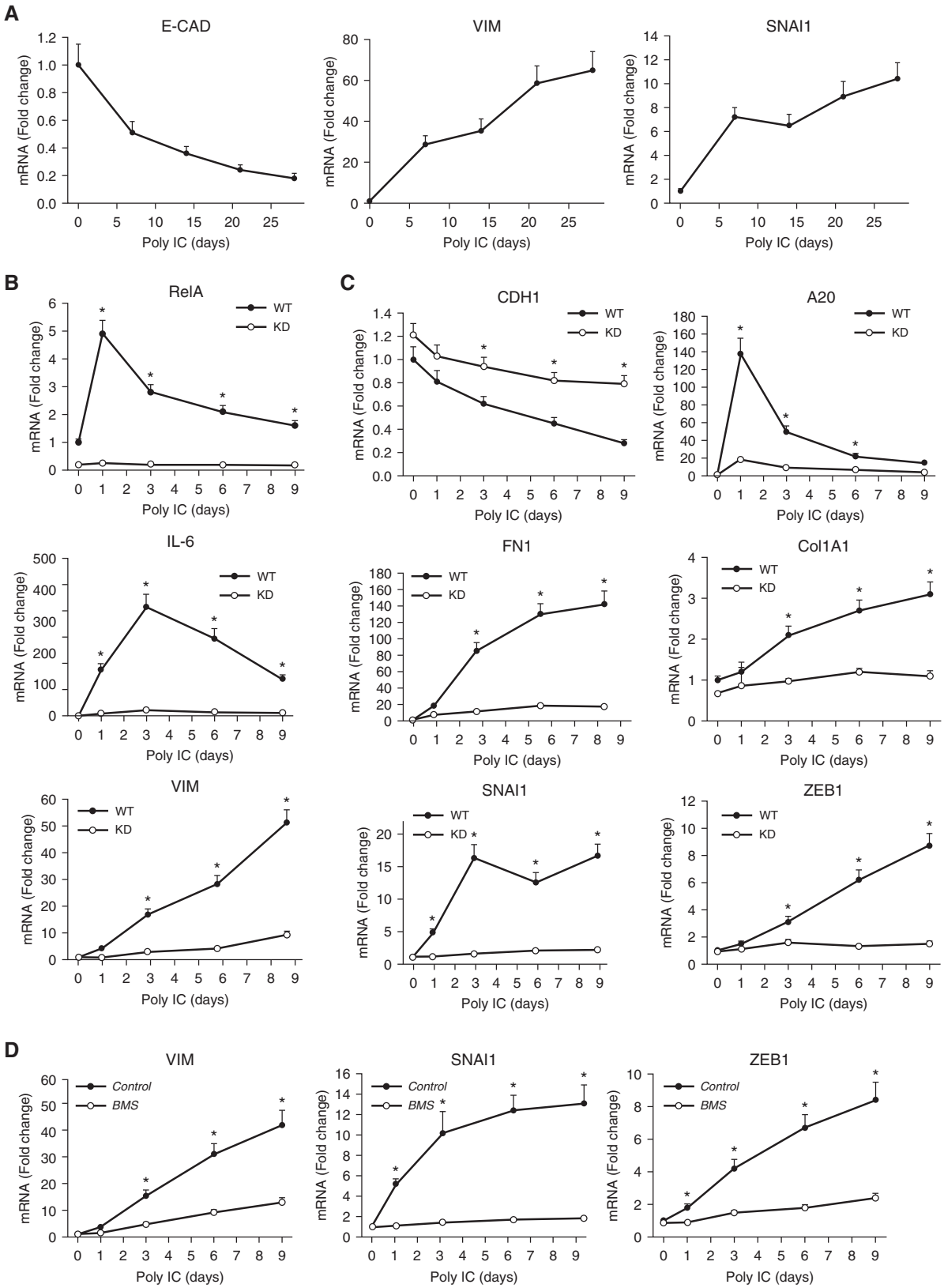

Figure 2. Poly(I:C) induces the mesenchymal program. (*A*) Repetitive poly(I:C) stimulation induces the epithelial–mesenchymal transition (EMT) gene program. hSAECs were stimulated with poly(I:C) 10 μg/ml for 1 hour daily. Afterwards, medium was replaced without poly(I:C). Shown is a time course for epithelial (E-CAD), mesenchymal (VIM), and EMT core regulator (SNAI1) gene expression. Data are representative of $n = 3$ time courses. *Note* the

(Dox)-inducible short hairpin RNA (shRNA). In the absence of RelA silencing, poly(I:C) rapidly induced *RelA* mRNA expression by 4.9-fold after 1 day of stimulation; this increased level of expression fell to twofold 9 days after poly(I:C) treatment (Figure 2B). Importantly, Dox treatment reduced endogenous *RelA* transcripts to less than 20% of that of wild-type cells (Figure 2B), persisting over 9 days of treatment, indicating a robust and persistent knockdown.

To examine whether this level of silencing interfered with the NF-κB expression program, RelA-shRNA hSAECs were poly(I:C) stimulated in the presence or absence of Dox, and changes in NF-κB–dependent genes measured by quantitative RT-PCR. In wild-type cells, poly(I:C) induced the NF-κB–dependent TNF alpha induced protein 3 (*TNFAIP3*)/*A20* gene by roughly 135-fold after 1 day, which monotonically fell to less than 20-fold after 9 days of stimulation. *TNFAIP3/A20* mRNA expression was significantly blocked by RelA silencing at all time points (Figure 2C). Poly(I:C) produced a 350-fold up-regulation of *IL-6*. Although the initial peak of up-regulated *IL-6* expression was slightly delayed relative to that of *TNFAIP3/A20*, RelA knockdown also significantly blocked poly(I:C)-induced NF-κB–dependent *IL-6* expression (Figure 2C). Together, these data indicate that the RelA shRNA silencing was functionally effective in blocking expression of its downstream genes.

We next examined the NF-κB dependence on poly(I:C)-induced expression of mesenchymal and fibrotic genes. In wild-type cells, *CDH1* mRNA expression fell to 80% after 1 day of poly(I:C) treatment, and continued to fall to approximately 30% 9 days after treatment (Figure 2C), a pattern consistent with the TGF-β–induced loss of differentiated epithelial marks (9). This inhibition was partially reversed by the RelA silencing, where *CDH1* mRNA levels fell to approximately 80% after 9 days of poly(I:C) treatment ($P < 0.01$, ANOVA). We also noted that the monophasic induction of the mesenchymal fibrotic genes, *FN1*, *COL1A1*, and *VIM*, by poly(I:C) over the course of stimulation was blocked by RelA silencing (Figure 2C). Finally, poly(I:C)-induced expression of mRNA of the core EMT regulators, *SNAI1* and *ZEB1*, was also blocked by RelA silencing. Consistent with our earlier observations of TGF-β–induced mesenchymal transition, *SNAI1* mRNA was the most rapidly and highly activated core EMT regulator, peaking within 3 days of stimulation at 17-fold over controls, whereas *ZEB1* mRNA exhibited a lower magnitude of induction (Figure 2C). Importantly, the poly(I:C) induction of *SNAI1* and *ZEB1* mRNA was significantly inhibited by RelA knockdown (Figure 2C).

To further explore the role of NF-κB pathway, hSAECs were treated in the absence or presence of an IKK inhibitor (BMS345541) and stimulated with poly(I:C) for up to 9 days. We observed that BMS345541 inhibited the poly(I:C)-induced expression of the *VIM* mesenchymal genes and *SNAI1* and *ZEB1* core EMT regulators (Figure 2D). Together, these data indicate the central role of the IKK–NF-κB/RelA pathway in poly(I:C)-induced mesenchymal transition in airway epithelial cells. These data indicate that chronic poly(I:C) stimulation induces the mesenchymal transition, and that the IKK–NF-κB/RelA pathway is upstream of the gene regulatory network controlling fibrosis.

Acute Exposure to Poly(I:C) Induces NF-κB–IKK–Dependent Neutrophilic Inflammation in Airways

We first determined the effect of IKK inhibition on acute poly(I:C)-induced airway neutrophilic inflammation. C57BL6/J mice pretreated with or without BMS345541 were challenged with intranasal poly(I:C). We observed that poly(I:C) induced a profound accumulation of neutrophils around the small- and medium-sized airways 24 hours after intranasal poly(I:C) challenge (Figure 3A) that was completely inhibited by BMS345541 administration. The total number of bronchoalveolar lavage fluid (BALF) cells increased nearly four times over that of PBS-treated mice, an induction completely inhibited by BMS345541 treatment (Figure 3B, *left panel*). In addition, the percentage of BALF neutrophils increased from 1 to 61.3% in PBS-treated mice exposed to poly(I:C), an effect reduced to 6.3% in BMS345541-treated mice (Figure 3B).

Correspondingly, poly(I:C) induced dramatic inductions of inflammatory cytokine levels measured in the BALF. In comparison to PBS-treated mice, IL-6 protein abundance was below the lower limit of detection (LLOD); poly(I:C) increased IL-6 from its LLOD to 632 pg/ml (Figure 3C). Similar poly(I:C)-induced expression patterns were seen for keratinocyte chemoattractant (KC), increasing to 791 pg/ml, monocyte chemoatractant protein-1 (MCP-1) to 4,962 pg/ml, granulocyte/macrophage colony–stimulating factor to 2,000 pg/ml, macrophage inflammatory protein-1β (MIP-1β) to 500 pg/ml, and regulated upon activation, normal T cell expressed and secreted to 1,793 pg/ml from their LLOD (Figure 3C). In the BMS345541-treated animals, poly(I:C)-induced values were reduced by over 95%, nearly to those of PBS-challenged mice (Figure 3C). Together, these data indicate that NF-κB is required for TLR3-induced activation of the innate immune response and airway neutrophilia.

Figure 2. (Continued). coordinate down-regulation of CDH1 and up-regulation of the mesenchymal transcripts. (*B*) Silencing NF-κB/RelA. hSAECs stably transfected with a doxycycline (Dox)-inducible lentivirus expressing RelA short hairpin RNA were cultured in the absence (wild type [WT]) or presence of Dox for 5 days to induce RelA knockdown (KD). Cells were then stimulated with poly(I:C) (10 μg/mL) up to 9 days. The expression of *RelA* mRNA is shown as the mean fold change in mRNA abundance (±SD) normalized to human cyclophilin (*hPPIA*). Data are from three independent experiments. *$P < 0.01$ ANOVA with Tukey's *post hoc t* test. (*C*) Effect of NF-κB/RelA silencing on the poly(I:C)-induced EMT gene expression program. RelA-expressing and RelA-silenced hSAECs were stimulated with poly(I:C) and expression of epithelial *CDH1*, NF-κB dependent genes (*TNF α induced protein 3* [*TNFAIP3*]/*A20* and *IL-6*), mesenchymal markers (*fibronectin* [*FN*] *1*, *VIM*, *collagen* [*COL*] *1A*), and core EMT transcriptional regulators (*SNAI1*, *zinc finger E-box binding homeobox* [*ZEB*] *1* and *Twist family BHLH transcription factor 1*) were determined. Shown is fold change mRNA abundance normalized to *hPPIA*. Data are means (±SD) from $n = 3$ independent experiments. *$P < 0.01$ ANOVA with *post hoc t* test. (*D*) Requirement of the IκB kinase in mesenchymal transition. hSAECs were stimulated with poly(I:C) in the absence or presence of BMS345541 (10 μM). mRNA expression of indicated genes were determined. Data are means (±SD) from $n = 3$ independent experiments. *$P < 0.01$ ANOVA with *post hoc t* test.

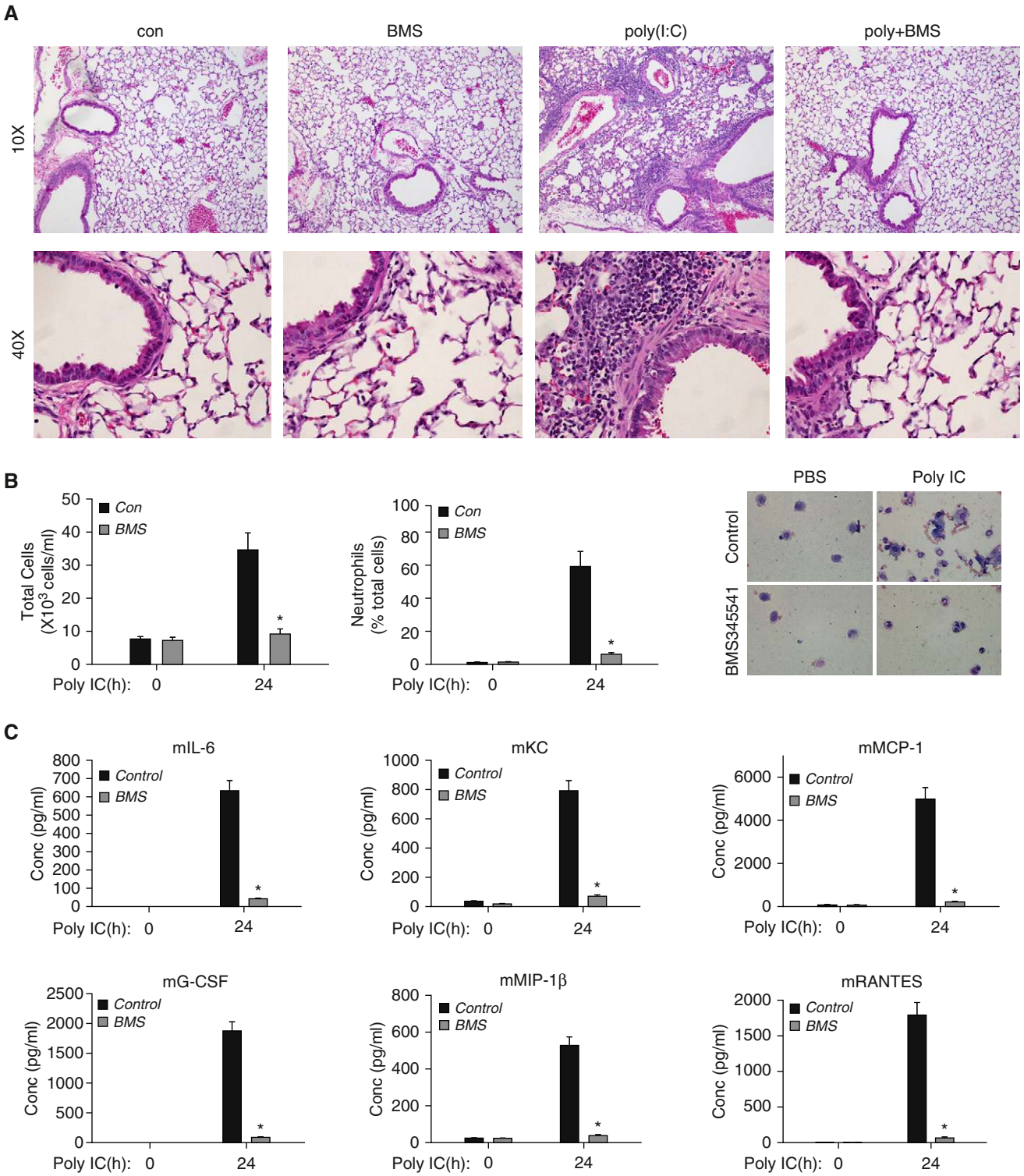

Figure 3. Poly(I:C) challenge–induced inflammation. C57BL6/J mice were pretreated with or without BMS345541 (BMS; 10 mg/kg) via the intraperitoneal route. After 24 hours, another dose of intraperitoneal BMS345541 was administered and mice were stimulated intranasally with either 50 μl of PBS or 50 μl PBS plus 500 μg poly(I:C) for 24 hours. (*A*) Hematoxylin and eosin (H&E) staining of paraffin-embedded mouse lung sections from acute poly(I:C)-challenged mice. *Top row*, 10× magnification; *bottom row*, 40× magnification. (*B*) Effect of BMS345541 on inflammatory cell recruitment into the bronchoalveolar lavage fluid (BALF). Cell counts are expressed as total number of cells × 10^3/ml. *$P < 0.05$ BMS345541 + poly(I:C) versus poly(I:C)-treated animals ($n = 5$ mice per group). *Middle*, percentage of neutrophils; *right*, cytospin preparations stained with H&E. (*C*) Effect of BMS345541 on BALF cytokine levels. Cytokines were measured

Chronic Poly(I:C) Treatment Induces Airway Remodeling and Pulmonary Fibrosis

Reasoning that persistent TLR3 activation induces EMT in hSAECs (Figures 1 and 2), and that EMT may be associated with airway remodeling, we asked whether repetitive TLR3 activation would produce airway remodeling/fibrosis *in vivo*. Mice were repetitively challenged with intranasal poly(I:C) for 15 challenges, followed by a 12-day rest period (Figure 4A). To assess the role of NF-κB–IKK pathway in the tissue response, parallel groups were treated with BMS345541 before intranasal poly(I:C) challenge. We observed that the poly(I:C)-challenged mice lost 25% body weight compared with PBS-challenged mice, an effect that was prevented by BMS345541 treatment (Figure 4B).

Micro–computed tomography (micro-CT) imaging was performed to evaluate the presence of remodeling/fibrosis. These micro-CT images revealed infiltrates of dense matter, predominately in the left lobes of chronic poly(I:C)-treated mice, whereas the lungs of poly(I:C)-challenged mice pretreated with BMS345541 showed density similar to that seen in controls (Figure 4C). Quantification of the percentage of dense sectional area of these mice revealed the same findings (Figure 4D). Three-dimensional (3D) reconstruction of the lung parenchyma showed loss of airspace in the left upper lobe and left lower lobe (Figure 4E). Representative lungs from each treatment group were scanned *ex vivo* under conditions that provided better dynamic contrast. These images demonstrated the normal airway structure in the lungs of PBS-treated mice, whereas, in chronic poly(I:C)-challenged mice, the airway structure showed significant pulmonary fibrosis in the medium and small airways (Figure 4F).

To quantitatively assess the degree of fibrosis in intact lungs, we used a tissue-clearing technique to optically clear lung tissue, coupled with application of second harmonic generation microscopy (SHGM), a nonlinear optical microscopy technique for visualization and quantification of COL accumulation in the tissue (Figure 5A). We found that chronic poly(I:C) challenge induced a sevenfold increase of COL accumulation around the airways as compared with that of PBS-treated mice. COL accumulation in airway of poly(I:C)-challenged mice pretreated with BMS345541 showed comparable COL content to those controls challenged with PBS (Figure 5B).

Using a tiling approach of SHGM images, we created a 3D volume map of COL distribution concentrating on small airways ranging from 100–300 mm in diameter. The 3D volume map demonstrates the poly(I:C)-induced COL accumulation throughout the interstitial space surrounding these small- and medium-sized airways (shown in *green*, Figure 5C). To further demonstrate global airway fibrosis biochemically, we quantified COL abundance by assaying hydroxyproline content in the whole lungs and BALF. Poly(I:C) administration induced an approximately twofold increase in both total lung and BALF hydroxyproline abundance, an increase completely blocked in the BMS345541-treated animals (Figure 5D). Together, the results of the SHGM, micro-CT scan, and whole-lung COL content analyses clearly indicate that chronic poly(I:C) treatment induces airway remodeling and pulmonary fibrosis *in vivo*, and its effect could be abolished by inhibition of the IKK–NF-κB pathway.

IKK-NF-κB Pathway Mediates Chronic Poly(I:C)-Induced Airway Remodeling and Fibrosis

Examination of histopathological changes using light microscopy indicated that repetitive poly(I:C) treatment induced marked subepithelial fibrosis with enhanced COL distribution throughout the parenchyma (Figure 6A, COL in *blue*). The epithelium was flattened with loss of its brush-border appearance, and there were enhanced numbers of glandular cells. At higher power, we observed expansion of mesenchymal supporting cells, suggesting expansion of the epithelial–mesenchymal trophic unit (EMTU; *black arrow*, Figure 6A) and thickening of the alveolar septae. By contrast, the lungs of animals treated with BMS345541 were histologically normal, consistent with our earlier micro-CT and SHGM analysis indicating that IKK inhibition effectively blocked poly(I:C)-induced airway fibrosis (Figure 6A). The average combined Ashcroft score in poly(I:C) treatment was 9 ($n = 5$ mice), indicating a moderate level of pulmonary fibrosis, whereas the combined Ashcroft score in poly(I:C)$^+$ BMS345441-treated mice was significantly lower, at a value of 1 ($P < 0.01$, $n = 5$, Figure 6B). Unlike what we found in acute poly(I:C) exposure, the number of BALF leukocytes were similar in all the treatment groups, indicating that the acute inflammation had subsided (Figure 6C).

The levels of IL-6, KC, and regulated upon activation, normal T cell expressed and secreted in BALF were induced in the poly(I:C)-treated mice, and reduced by BMS345541 treatment (Figure 6D). There were no changes in MCP-1 (Figure 6D). We also noted that these cytokine levels were significantly lower than that of mice in response to acute poly(I:C) exposure (*compare* Figures 3 and 6D), indicating that chronic poly(I:C) challenge induced activation of the innate immune response, and that neutrophilia had largely abated during the 12-day rest period incorporated in to our experimental design (Figure 4A).

IKK-NF-κB Pathway Mediates Chronic Poly(I:C) Treatment–Induced EMT

To more precisely determine the presence of EMT and effect of BMS345541 on this process, IF stainings for the mesenchymal markers, SNAI1, VIM, COL1A, and FN1, were conducted. Only faint staining of SNAI1, VIM, FN1, and COL1A was detected in control airways (Figure 7A and Table 1). In contrast, chronic poly(I:C) induced enhanced staining of SNAI1, VIM, FN1, and COL1A (Figure 7A, *third row*). Importantly, IF staining for SNAI1 and FN1 were mainly enhanced in the epithelial surface, consistent with EMT formation. Furthermore, VIM and COL1A were more widely distributed throughout the interstitium. The expression of all of these mesenchymal markers were blocked by BMS345541 treatment (Figure 7A, *fourth row*), providing further evidence that IKK inhibition effectively blocks chronic poly(I:C)-induced mesenchymal transition, and links this program to pulmonary fibrosis.

Figure 3. (Continued). using multiplex ELISA ($n = 5$ mice/group). Protein concentration (pg/ml) was determined by reference to internal standards. *$P < 0.01$. Data are means (±SD) for $n = 5$ animals for each group. G-CSF, granulocyte-colony stimulating factor; KC, keratinocyte chemoattractant; m, mouse; MCP, monocyte chemotractant protein; MIP, macrophage inflammatory protein; RANTES, regulated upon activation, normal T cell expressed and secreted.

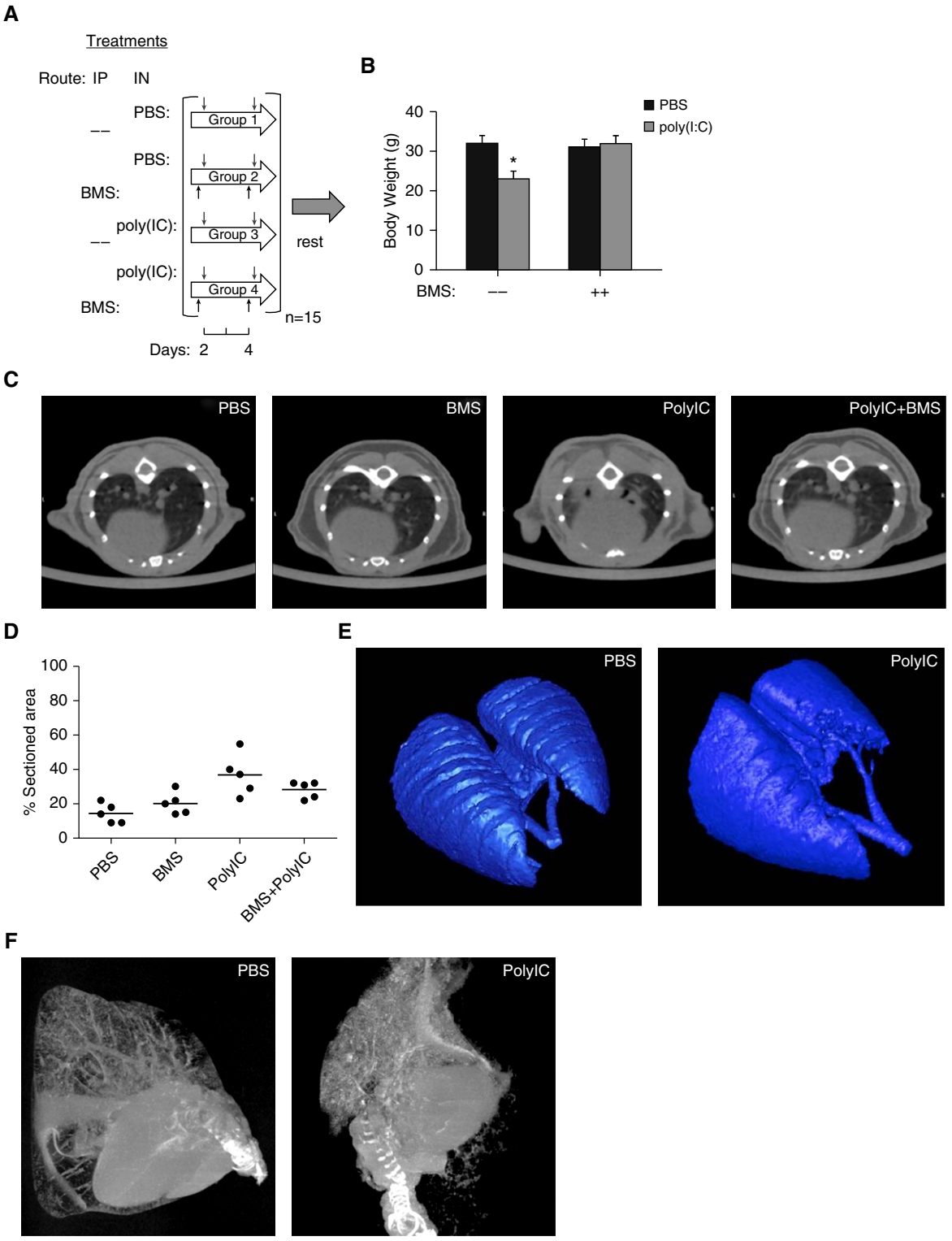

Figure 4. Quantification of airway fibrosis. (*A*) Schematic of experimental strategy. BMS345541- or vehicle-pretreated mice were subjected to 15 challenges with intranasal poly(I:C). At 12 days after the last challenge, mice were killed and analyzed. IN, intranasal administration; IP, intraperitoneal injection. (*B*) Effect of poly(I:C) on body weight. Body weight (g) in mice from each experimental group. Shown is mean (±SD) from $n = 5$ animals. $^*P < 0.05$ compared to PBS treatment alone. (*C*) Computed tomography (CT) axial images. Shown is plane at T6 level from a representative animal. *Note* the dense segmental fibrosis in the left lower lobe of the poly(I:C)-treated mouse. (*D*) Sectioned dense area as a fraction of lung area in images (*dots*) and mean value (*lines*). Threshold value is −200 Hounsfield units. (*E*) Three-dimensional (3D) reconstruction. Reconstruction of micro-CT from PBS- and poly(I:C)-treated mice from images obtained *in vivo*. (*F*) High-resolution reconstruction. Shown is 3D reconstruction of micro-CT imaging from heart–lung preparation from control (PBS) or poly(I:C)-treated mouse imaged *ex vivo*.

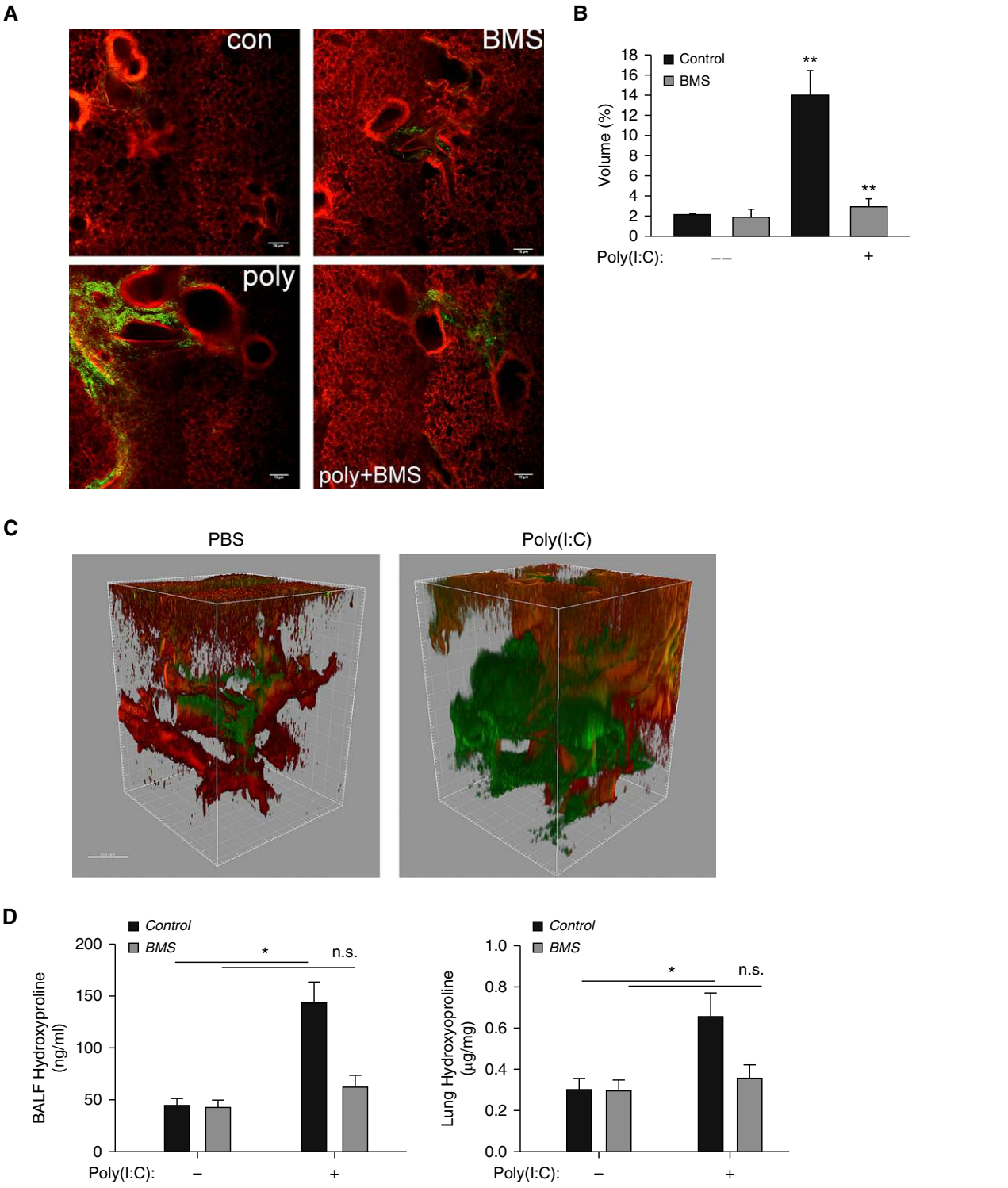

Figure 5. Visualization of COL accumulation via SHGM. (*A*) Two-photon cross-sections showing COL deposition around airways in PBS, poly(I:C), BMS345541, and BMS345541 + poly(I:C) groups. Contrast provided by tissue autofluorescence (*red*) and SHGM signal (*green*). Four fields of view taken at 25× stitched together, as described in the main text. (*B*) Percent area covered by COL calculated from total area covered by SHGM signal compared with total area imaged. One-way ANOVA was performed followed by Tukey's *post hoc* test to determine significance. $^{**}P < 0.01$ was considered significant. (*C*) 3D reconstructions of PBS and poly(I:C) groups. Coloring for autofluorescence and SHGM signal are as in *A*. (*D*) COL content. Hydroxyproline was quantified in whole lung and BALF. $^{*}P < 0.05$ for each pairwise comparison shown. Data are mean (±SD) for $n = 5$ animals for each group. *Scale bars*, 300 μm. COL, collagen; n.s., not significant; SHGM, second harmonic generation microscopy.

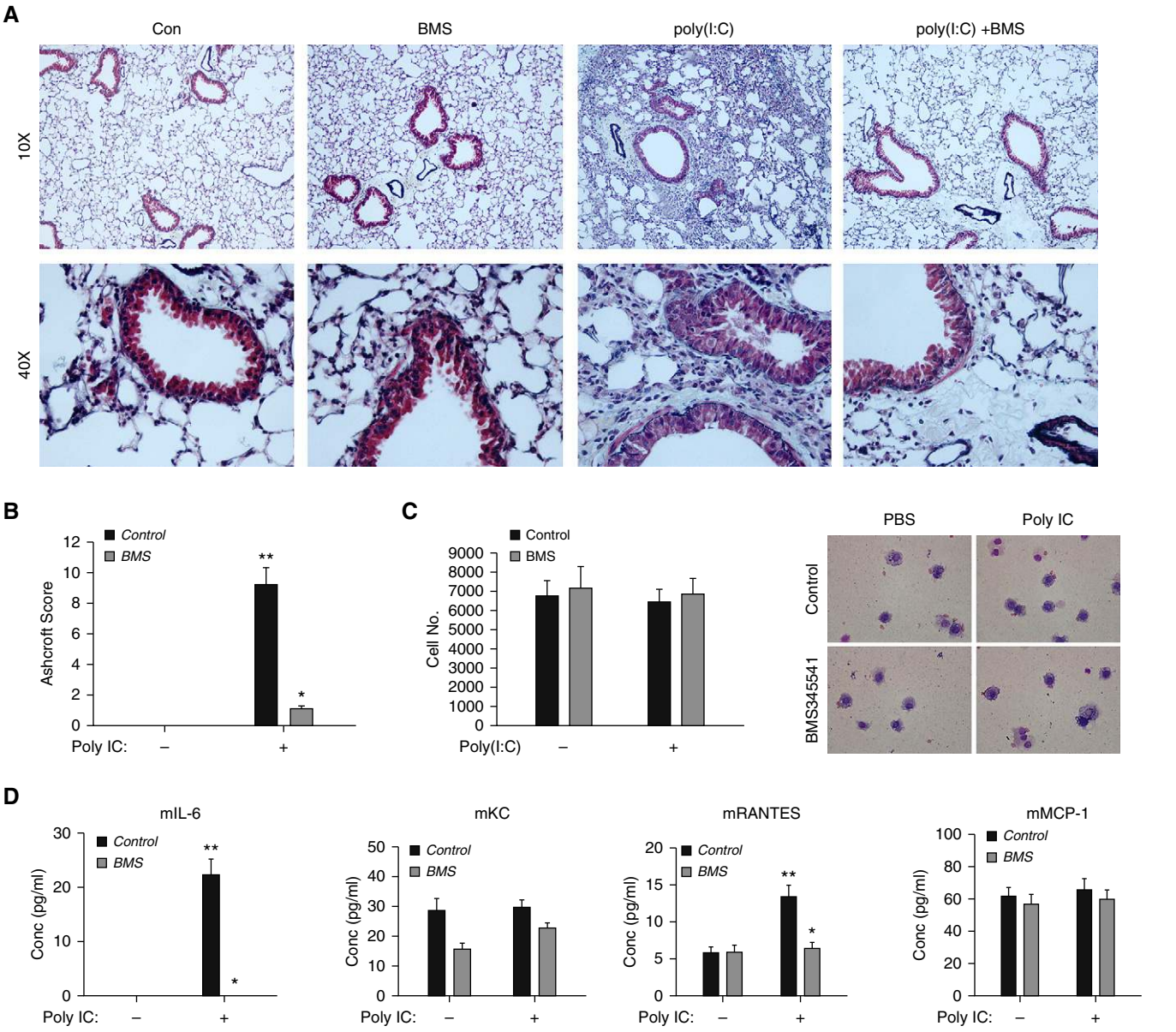

Figure 6. Histopathology and BALF analysis. C57BL6/J mice (18 wk old) were pretreated with and without BMS345541 (10 mg/kg body weight, intraperitoneal) and given repetitive intranasal challenges with poly(I:C) (500 μg/mouse every other day for 30 d). (*A*) Morphological changes after Masson trichrome staining. *Top row*, representative images at ×10; *bottom row*, images at ×40. *Note* the expansion of myofibroblasts in the poly(I:C) images at 40×. (*B*) The level of lung fibrosis was assessed using the Ashcroft scoring method. $^{*}P < 0.05$ for fibrosis scores of animals treated with BMS345541 compared to those without inhibitor. $^{**}P < 0.05$ for fibrosis scores of animals treated with poly(I:C) compared to controls. (*C*) Effect of BMS345541 on cellular recruitment in BALF. Cell counts in the BALF expressed as total number of cells × 10^3/ml. No statistical differences were observed in poly(I:C) treatment or BMS345541 groups ($n = 5$ mice/group). (*D*) Effect of BMS345541 on cytokine secretion in BALF. BALF was analyzed for cytokines using multiplex ELISA ($n = 5$ mice/group). Protein concentration (pg/ml) was determined by reference to internal standards. $^{*}P < 0.01$ poly(I:C) + vehicle versus poly(I:C) + BMS345541; $^{**}P < 0.01$ compared to PBS treatment alone. Data are mean (±SD) for $n = 5$ animals for each group.

At the molecular level, repetitive poly(I:C) stimulation induced the expression of NF-κB–dependent genes (*RelA*, *KC*, *IL-6*) and mesenchymal genes (*SNAI1*, *FN-1*, *VIM*, *COL1A1*) in total lung RNA (Figure 7B). BMS345541 treatment significantly inhibited the chronic poly(I:C)-induced pulmonary fibrotic program (Figure 7B). Together, our mechanistic studies using cultured cells and animal models have identified NF-κB as a key regulator of chronic poly(I:C)-induced airway fibrosis and remodeling, providing a new model and pathway for therapeutic intervention for chronic airway disease–associated pulmonary fibrosis (Figure 7C).

Discussion

The results of our studies indicate an association of chronic activation of the NF-κB pathway downstream of TLR3

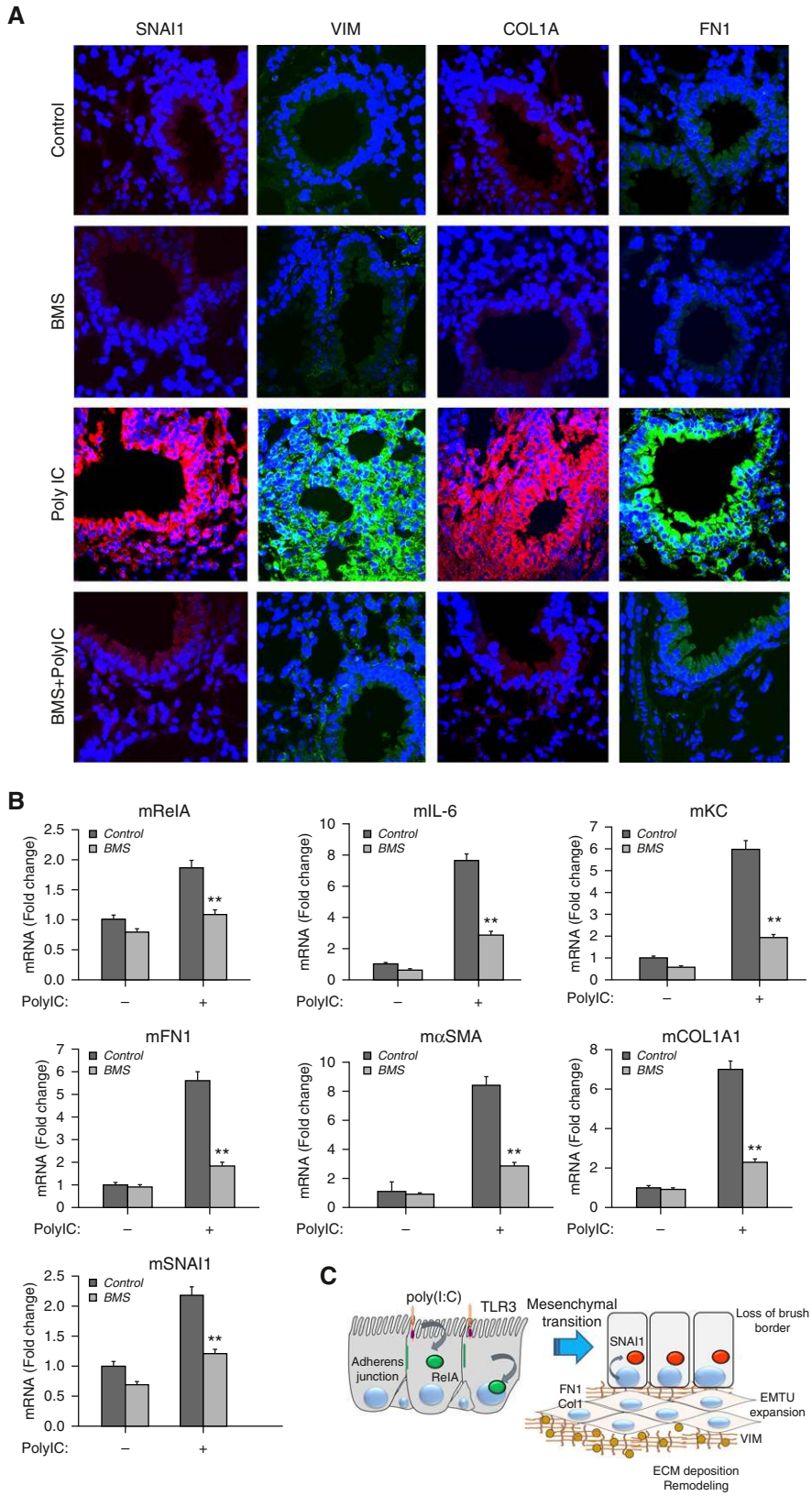

Figure 7. Repetitive poly(I:C) induces EMT program *in vivo*. (*A*) Induction of the mesenchymal program in airway epithelium. Lung sections were fixed, permeabilized, and incubated with IgG or anti-COL1A, VIM, FN1, or SNAI1 Abs, then stained with AlexaFluor488- or AlexaFluor568-conjugated

signaling with EMT, airway remodeling, and fibrosis. In support, we observed that poly(I:C) activated expression of the core mesenchymal transcriptional regulators, SNAI1 and ZEB1, as well as fibrotic program in a manner dependent on the IKK–NF-κB pathway, by normal hSAECs. Correspondingly, repetitive poly(I:C) challenge induces dramatic morphological changes in the epithelium and expansion of subepithelial mesenchymal cells, with enhanced COL deposition in the medium and small airways (Figure 5). Linking our cellular studies with the complex responses in the animal model, we observed enhanced expression of SNAI1 and FN1 in the airway epithelial layer, providing evidence that poly(I:C) induces features of the mesenchymal transition that may be associated with airway remodeling (Figure 7C). Our results further indicate that the weight loss, cellular remodeling, EMT, and fibrosis induced by poly(I:C) were blocked by BMS345541 treatment, consistent with the conclusion that NF-κB is required for EMT-associated lung remodeling. Together, these data provide insight into the potential mechanisms as to how repetitive viral infections can be linked to airway fibrosis, through the IKK–NF-κB pathway.

Using an *in vitro* model of telomerase-immortalized epithelial cells, we have found that NF-κB/RelA is a master mediator of TGF-β–induced EMT (9, 21). Mechanistically, we know that TGF-β activates NF-κB/RelA through a complex mechanism, initially producing activating serine 276 phosphorylation, followed by the later production of a paracrine factor inducing its translocation through the canonical pathway (28). In the nucleus, NF-κB/RelA directly up-regulates the core EMT regulators, including SNAI1, Twist family BHLH transcription factor 1, and ZEB1, by binding to their proximal promoter regions and activating their expression by a transcriptional elongation mechanism (28). hSAECs have many characteristics of primary epithelial cells, in particular the innate pathway coupled to NF-κB activation, and the fact that these features are observed *in vivo*. Although the NF-κB pathway is highly conserved across epithelial types, our studies linking chronic poly(I:C) activation to mesenchymal transition will need to be validated in future studies with other primary airway epithelial cell types.

Table 1. Sequences of PCR Primers for Quantitative RT-PCR

Primer Set	Sequence (5′–3′)	
	Forward	Reverse
hRelA	CCGGACCGCTGCATCCACAG	AGTCCCCACGCTGCTCTTCT
hFN1	CGGTGGCTGTCAGTCAAAG	AAACCTCGGCTTCCTCCATAA
hCOL1A	CCAGAAGAACTGGTACATCAGCA	CGCCATACTCGAACTGGAATC
hIL-6	CTGGATTCAATGAGGAGACTTGC	TCAAATCTGTTCTGGAGGTACTCTAGG
hSNAI1	GCGCTCTTTCCTCGTCAGG	GGGCTGCTGGAAGGTAAACTCT
hTWIST1	TCTCGGTCTGGAGGATGGA	CAATGACATCTAGGTCTCCG
hVIM	GCTCAATGTTAAGATGGCCCTT	TGGAAGAGGCAGAGAAATCCTG
hZEB1	GATGATGAATGCGAGTCAGATGC	GATGATGAATGCGAGTCAGATGC
hTNFAIP3	TCCTCAGGCTTTGTATTTGAGC	TGTGTATCGGTGCATGGTTTTA
hCDH1	CGAGAGCTACACGTTCACGG	GGGTGTCGAGGGAAAAATAGG
hPPIA	CCCACCGTGTTCTTCGACATT	GGACCCGTATGCTTTAGGATGA
mIL-6	TAGTCCTTCCTACCCCAATTTCC	TTGGTCCTTAGCCACTCCTTC
mSNAI1	CACACGCTGCCTTGTGTCT	GGTCAGCAAAAGCACGGTT
mRelA	AGGCTTCTGGGCCTTATGTG	TGCTTCTCTCGCCAGGAATAC
mCOL1A1	GCTCCTCTTAGGGGCCACT	CCACGTCTCACCATTGGGG
mVIM	CGTCCACACGCACCTACAG	GGGGGATGAGGAATAGAGGCT
mαSMA	GTCCCAGACATCAGGGAGTAA	TCGGATACTTCAGCGTCAGGA
mFN1	ATGTGGACCCCTCCTGATAGT	GCCCAGTGATTTCAGCAAAGG
mKC	CTGGGATTCACCTCAAGAACATC	CAGGGTCAAGGCAAGCCTC
mPPIA	GAGCTGTTTGCAGACAAAGTTC	CCCTGGCACATGAATCCTGG

Definition of abbreviations: αSMA, α smooth muscle actin; CDH, E-cadherin; COL, collagen; FN, fibronectin; h, human; KC, keratinocyte chemoattractant; m, mouse; PPIA, cyclophilin; SNAI1, Snail family zinc finger; TNFAIP, TNF-α induced protein; TWIST, Twist family BHLH transcription factor 1; VIM, vimentin; ZEB, zinc finger E-box binding homeobox.

Although the proinflammatory cytokines, IL-1β, TNFs, and IFNs, have been shown to modulate TGF-β–induced EMT (29), none of these proinflammatory factors by themselves produces a stable type II EMT. We report, for the first time, that persistent activation of the IKK–NF-κB pathway by viral patterns is sufficient to trigger EMT in cultured hSAECs. Our demonstration that poly(I:C) up-regulates the core regulators, *SNAI1*, *ZEB1*, and mesenchymal *VIM* and *FN1* genes, suggests that poly(I:C)–TLR3 signaling activates gene regulatory networks shared with those induced by TGF-β in the prototypical EMT program.

We interpret the robust SNAI1 and FN1 expression–associated enhanced extracellular matrix deposition and myofibroblast transition associated with enhanced interstitial VIM staining to indicate that poly(I:C) induces molecular features of an EMT state *in vivo*. These chronic inflammatory responses resemble those features of mesenchymal transition observed in bronchial epithelium in patients with severe asthma and COPD (7, 9, 14, 30). In our repetitive inflammation model, poly(I:C) directly activates epithelial cells, because these cells constitutively express cell-surface TLR3 (31). More work will be required to examine the role of the epithelium in fibrosis and remodeling.

Airway Fibrosis in Response to Poly(I:C)

Our multimodal imaging studies using micro-CT, a well established approach for quantitative assessment of pulmonary fibrosis (32), SHGM to measure 3D COL deposition patterns, and tissue clearing all indicate that the pattern of fibrosis associated with repetitive poly(I:C) stimulation is heterogeneous. This fibrosis involves the small- and medium-sized airspaces, and is primarily concentrated in the left lung. One explanation for this asymmetric distribution may be anatomical—with the left lung being smaller and less lobulated than the right, enabling intranasal poly(I:C) to preferentially distribute to this side. We note that patterns of bleomycin-induced fibrosis are dependent on its route of administration as well (33). Our cell culture analysis indicates that poly(I:C) induces a fibrotic gene expression program, including up-regulation of *COL1A* and *FN1*, genes the expression of which are both enhanced in the lung. These observations suggest that the epithelium may play multiple roles in poly(I:C)-induced fibrosis—directly, by producing COL1A and FN1, and indirectly through secretion of factors that activate myofibroblasts. Of relevance,

Figure 7. (Continued). goat anti-rabbit IgG (shown in *green* or *red*, respectively), counterstained with DAPI, and imaged via fluorescence microscopy. (*B*). Analysis of the fibrotic and EMT program. Total lung RNA was extracted, purified, and reverse transcribed. The abundance of indicated mRNAs was determined using mouse gene–selective primers (Table 1). Shown is mean fold change mRNA abundance (±SD) normalized to mouse cyclophilin (*mPPIA*) for $n = 5$ animals from each treatment group. (*C*) Mechanistic linkage of NF-κB activation with mesenchymal transition and airway remodeling. Shown is a schematic model of airway epithelium stimulated with TLR3 agonist. Persistent activation of the NF-κB pathway results in up-regulation of the core EMT regulator SNAI1, as well as enhanced production of extracellular matrix proteins FN1 and Col1A. Expansion of myofibroblast population is indicated by interstitial VIM up-regulation and accumulation of hydroxyproline. Down-regulation of CDH1 results in reduced adherens junctions and enhanced epithelial permeability. $^{**}P < 0.01$ compared to poly(I:C) + vehicle treated mice. ECM, extracellular matrix; EMTU, epithelial–mesenchymal trophic unit; TLR3, Toll-like receptor 3.

we have recently shown that lower airway epithelial cells have distinct patterns of secreted proteins from RNA viral infections (24); localization of fibrosis to the small- and medium-sized airways may be partly due to distinct lower airway cell responses.

Potential Role of the Epithelium in Poly(I:C)-Induced Remodeling

Our histological studies indicate that poly(I:C) induces broad effects on the airway mucosa, including morphological changes in the epithelium (bronchial epithelial flattening, loss of the brush border), enhanced appearance of glandular cells, as well as expansion of subepithelial fibroblast populations. Epithelial cells constitutively express TLR3 receptors, and consequently respond to extracellular poly(I:C) *in vitro* (20) and *in vivo* (31). In our chronic poly(I:C) model, we also think that expansion of the myofibroblast population is seen; this is suggested by an expanded population of subepithelial mesenchymal cells (Figure 6A), cells that express VIM (Figure 7A). These findings indicate that poly(I:C) activates expansion of the EMTU. Under normal conditions, the EMTU is only a thin layer of subepithelial mesenchymal cells (34). By contrast, in response to epithelial injury and acute inflammation, the EMTU dynamically expands to assume a secretory phenotype characteristic of myofibroblasts, enhancing subepithelial matrix deposition (35). Myofibroblast expansion occurs partly in response to intercellular signals released from injured epithelial cells, such as growth factors (TGF-β and epidermal growth factor) and cytokines (periostin, IL-11, IL-17) that promote proliferation, transdifferentiation, and synthesis of extracellular matrix (36). EMTU expansion may also be the consequence of NF-κB signaling to trigger the IL-6 growth factor (9, 21, 28). More studies will be required to understand the mediators of mesenchymal expansion in this model. We interpret these observations and literature to mean that epithelial cell state responses may play a central role in the poly(I:C)-induced fibrotic program. Our studies were not designed to identify the origin of the mesenchymal fibroblast population; other studies suggest these may arise from mesenchymal transition of epithelial cells (37), circulating mesenchymal stem cells, or myofibroblast transition of resident fibroblasts (38).

In addition to the expansion of the myofibroblast population, we observed increased numbers of secretory cells, implicating the presence of goblet cell metaplasia, a process that results from transdifferentiation of ciliated epithelial and Clara cells to mucus-producing goblet cells. Chronic epithelial stimulation with TGF and amphiregulin are thought to be responsible for goblet cell metaplasia (36). How innate signaling or mesenchymal transition is linked to stem cell expansion and induction of epithelial transdifferentiation programs underlying goblet cell hyperplasia will be of interest to pursue in future studies.

Differences in Response to Acute versus Chronic Mucosal Stimulation

There are few studies available examining the effects of chronic inflammation on airway responses. A potentially important and interesting finding from our study was that repetitive poly(I:C) stimulation, mimicking repeated viral infections, reprograms mucosal signal transduction pathways. Although it has been widely observed that acute poly(I:C) produces a robust inflammatory and antiviral response (20), our studies here show that chronic poly(I:C) stimulation results in a later gene expression program that resembles TGF-β–induced mesenchymal transition and fibrosis. How could chronic inflammation produce a different response than an acute stimulation? One insight generated using systems-level approaches developed by our group is that the mesenchymal transition *itself* reprograms intracellular signaling pathways (39). Mechanistically, this is the result of dramatic changes in kinome and phosphatase expression patterns (40) as a result of the epigenetic reprogramming induced by the transition (9, 13). Studies on how this mesenchymal transition affects responses to viral RNA patterns are needed. These data are consistent with our previous work, showing that the airway mucosa expression program evolves from an acute inflammation to chronic fibrosis after chronic oxidative DNA damage (41). We note that TLR3 is also a potent activator of reactive oxygen species signaling (42), and potentially suggests a role for reactive oxygen species in airway fibrosis, the understanding of which will require further investigation.

Role of Leukocytic Inflammation in Poly(I:C)-Induced Fibrosis

In vivo, poly(I:C) induces perivascular/peribronchiolar inflammatory infiltrates due to increased cytokine production (22). Long-term activation of TLR3 by poly(I:C) induces inflammation and impairs lung function in mice (43), features characteristic of acute viral infections (44). Neutrophil recruitment is a hallmark of the innate immune response, mediated by release of epithelial-derived chemokines and danger patterns. Of relevance here, NF-κB–driven expression of chemokines, such as CXCL, KC, and granulocyte/macrophage colony–stimulating factor, enhance neutrophil recruitment and survival. Our data suggest that neutrophil-secreted proteases may play important roles in viral pattern–induced airway remodeling. Although we observed persistent elevation of IL-6 at 12 days after the last poly(I:C) challenge, our study was not designed to reveal how changes in profiles of cytokine responses occur after serial challenge.

Relation of Inflammation-Induced Fibrosis to Other Lung Fibrosis Models

Although others have shown that ectopic expression of IL-1 and TNF is sufficient to produce airway fibrosis, a clinically relevant model of viral RNA pattern–induced airway fibrosis has not yet been reported to our knowledge. The gold standard for airway fibrosis has been the bleomycin animal model (45). The response to bleomycin is typically characterized by acute injury associated with endothelial cell injury and loss of type 1 epithelial cells, followed by proliferation of fibroblasts and the presence of alveolar debris, resulting in inflammation, edema, and release of mediators/inflammatory components. In its final stages, increases in airway neutrophil and lymphocyte numbers (46), disturbed alveolar structure, accumulation of COL around alveoli, up-regulated expression of COL, and an increase in plasma TGF-β levels result in remodeling and airspace destruction (47). Although both chronic poly(I:C) and bleomycin models converge on the TGF-β signaling pathway, the initial effect of bleomycin is not via TLR3-

mediated signaling, but rather through a toxic response mediated by free-radical formation, cell death, and stromal expansion of fibroblasts (48). Thus, the applicability of understanding of the EMT and airway remodeling responses in the bleomycin model may be limited.

Relevance of the Model of Chronic Innate Inflammation to Human Airway Disease

Our model of chronic innate inflammation secondary to TLR3-associated stimulation is related to the effect of repetitive airway viral infections. Viral respiratory infections trigger acute innate responses in the airways and are associated with acute respiratory decompensations in patients with underlying asthma (49), COPD (50), and cystic fibrosis (51). In particular, infections with the paramyxovirus and respiratory syncytial virus (which occur repeatedly throughout life), are linked to decompensation of airway function and remodeling (17). Similarly, prospective observational studies have demonstrated that frequent respiratory infections are linked to persistent IL-6 expression, neutrophilia, and declines in forced expiratory volume in 1 second in COPD (52). We also note that weight loss, a prominent manifestation of our mouse model, is a significant comorbidity in COPD associated with systemic inflammation and cachexia (53). Thus, our data support that models of viral infection associated with inflammation-induced airway remodeling and fibrosis are important for understanding the pathogenic mechanisms of viral-induced exacerbation of obstructive lung diseases and mediators of cachexia.

Conclusions

Airway remodeling is a multicellular process that causes a progressive decline of pulmonary function. Tissue remodeling has been associated with respiratory virus infections, of which the mechanism(s) is largely unknown. We investigated the effects of persistent activation of the innate immune response on mesenchymal transition in normal airway epithelial cells and *in vivo*. *In vitro*, extracellular poly(I:C) triggered an epithelial cell state change characteristic of EMT that was absolutely dependent on activity of the IKK–NF-κB/RelA pathway. *In vivo*, repetitive activation of TLR3 produced NF-κB/RelA–dependent airway remodeling, expansion of the EMTU, mesenchymal transition of epithelial surface, and fibrosis of the proximal and small airways. The consistency of those data across our *in vitro* and *in vivo* investigations indicate that this model may be useful for analyzing the role of epithelium in inflammation-induced airway fibrosis and cachexia. ■

Author disclosures are available with the text of this article at www.atsjournals.org.

References

1. Akinbami LJ, Moorman JE, Bailey C, Zahran HS, King M, Johnson CA, Liu X. Trends in asthma prevalence, health care use, and mortality in the United States, 2001–2010. *NCHS Data Brief* 2012;(94):1–8.
2. Al-Muhsen S, Johnson JR, Hamid Q. Remodeling in asthma. *J Allergy Clin Immunol* 2011;128:451–462; quiz 463–454.
3. Wedzicha JA. Role of viruses in exacerbations of chronic obstructive pulmonary disease. *Proc Am Thorac Soc* 2004;1:115–120.
4. Harris WT, Kelly DR, Zhou Y, Wang D, MacEwen M, Hagood JS, Clancy JP, Ambalavanan N, Sorscher EJ. Myofibroblast differentiation and enhanced TGF-B signaling in cystic fibrosis lung disease. *PLoS One* 2013;8:e70196. [Published erratum appears in *PLoS One* 8.]
5. Fedorov IA, Wilson SJ, Davies DE, Holgate ST. Epithelial stress and structural remodelling in childhood asthma. *Thorax* 2005;60: 389–394.
6. Noble PW, Barkauskas CE, Jiang D. Pulmonary fibrosis: patterns and perpetrators. *J Clin Invest* 2012;122:2756–2762.
7. Holgate ST, Holloway J, Wilson S, Bucchieri F, Puddicombe S, Davies DE. Epithelial–mesenchymal communication in the pathogenesis of chronic asthma. *Proc Am Thorac Soc* 2004;1:93–98.
8. Aysola RS, Hoffman EA, Gierada D, Wenzel S, Cook-Granroth J, Tarsi J, Zheng J, Schechtman KB, Ramkumar TP, Cochran R, *et al*. Airway remodeling measured by multidetector CT is increased in severe asthma and correlates with pathology. *Chest* 2008;134: 1183–1191.
9. Ijaz T, Pazdrak K, Kalita M, Konig R, Choudhary S, Tian B, Boldogh I, Brasier AR. Systems biology approaches to understanding epithelial mesenchymal transition (EMT) in mucosal remodeling and signaling in asthma. *World Allergy Organ J* 2014;7:13.
10. Vincent T, Neve EP, Johnson JR, Kukalev A, Rojo F, Albanell J, Pietras K, Virtanen I, Philipson L, Leopold PL, *et al*. A SNAIL1-SMAD3/4 transcriptional repressor complex promotes TGF-beta mediated epithelial–mesenchymal transition. *Nat Cell Biol* 2009;11:943–950.
11. Kalluri R, Weinberg RA. The basics of epithelial–mesenchymal transition. *J Clin Invest* 2009;119:1420–1428.
12. Knight DA, Holgate ST. The airway epithelium: structural and functional properties in health and disease. *Respirology* 2003;8:432–446.
13. Kalita M, Tian B, Gao B, Choudhary S, Wood TG, Carmical JR, Boldogh I, Mitra S, Minna JD, Brasier AR. Systems approaches to modeling chronic mucosal inflammation. *BioMed Res Int* 2013;2013: 505864.
14. Wang Q, Wang Y, Zhang Y, Zhang Y, Xiao W. The role of uPAR in epithelial–mesenchymal transition in small airway epithelium of patients with chronic obstructive pulmonary disease. *Respir Res* 2013;14:67.
15. Bousquet J, Jeffery PK, Busse WW, Johnson M, Vignola AM. Asthma: from bronchoconstriction to airways inflammation and remodeling. *Am J Respir Crit Care Med* 2000;161:1720–1745.
16. Hogg JC, Chu F, Utokaparch S, Woods R, Elliott WM, Buzatu L, Cherniack RM, Rogers RM, Sciurba FC, Coxson HO, *et al*. The nature of small-airway obstruction in chronic obstructive pulmonary disease. *N Engl J Med* 2004;350:2645–2653.
17. Johnston SL. Innate immunity in the pathogenesis of virus-induced asthma exacerbations. *Proc Am Thorac Soc* 2007;4:267–270.
18. Matsumoto K, Inoue H. Viral infections in asthma and COPD. *Respir Investig* 2014;52:92–100.
19. O'Byrne PM, Pedersen S, Lamm CJ, Tan WC, Busse WW; START Investigators Group. Severe exacerbations and decline in lung function in asthma. *Am J Respir Crit Care Med* 2009;179:19–24.
20. Bertolusso R, Tian B, Zhao Y, Vergara L, Sabree A, Iwanaszko M, Lipniacki T, Brasier AR, Kimmel M. Dynamic cross talk model of the epithelial innate immune response to double-stranded RNA stimulation: coordinated dynamics emerging from cell-level noise. *PLoS One* 2014;9:e93396.
21. Tian B, Li X, Kalita M, Widen SG, Yang J, Bhavnani SK, Dang B, Kudlicki A, Sinha M, Kong F, *et al*. Analysis of the TGFβ-induced program in primary airway epithelial cells shows essential role of NF-κB/RelA signaling network in type II epithelial mesenchymal transition. *BMC Genomics* 2015;16:529.
22. Stowell NC, Seideman J, Raymond HA, Smalley KA, Lamb RJ, Egenolf DD, Bugelski PJ, Murray LA, Marsters PA, Bunting RA, *et al*. Long-term activation of TLR3 by poly(I:C) induces inflammation and impairs lung function in mice. *Respir Res* 2009;10:43.
23. Ramirez RD, Sheridan S, Girard L, Sato M, Kim Y, Pollack J, Peyton M, Zou Y, Kurie JM, Dimaio JM, *et al*. Immortalization of human bronchial epithelial cells in the absence of viral oncoproteins. *Cancer Res* 2004;64:9027–9034.

24. Tian B, Yang J, Zhao Y, Ivanciuc T, Sun H, Garofalo RP, Brasier AR. Bromodomain containing 4 (BRD4) couples NFκB/RelA with airway inflammation and the IRF-RIG-I amplification loop in respiratory syncytial virus infection. *J Virol.* [online ahead of print] 11 Jan 2017; DOI: 10.1128/JVI.00007-17.
25. Vaughan MB, Ramirez RD, Wright WE, Minna JD, Shay JW. A three-dimensional model of differentiation of immortalized human bronchial epithelial cells. *Differentiation* 2006;74:141–148.
26. Delgado O, Kaisani AA, Spinola M, Xie XJ, Batten KG, Minna JD, Wright WE, Shay JW. Multipotent capacity of immortalized human bronchial epithelial cells. *PLoS One* 2011;6:e22023.
27. Kaisani A, Delgado O, Fasciani G, Kim SB, Wright WE, Minna JD, Shay JW. Branching morphogenesis of immortalized human bronchial epithelial cells in three-dimensional culture. *Differentiation* 2014;87: 119–126.
28. Tian B, Zhao Y, Sun H, Zhang Y, Yang J, Brasier AR. BRD4 mediates NFκB-dependent epithelial–mesenchymal transition and pulmonary fibrosis via transcriptional elongation. *Am J Physiol Lung Cell Mol Physiol* 2016;311:L1183–L1201.
29. Wu Y, Deng J, Rychahou PG, Qiu S, Evers BM, Zhou BP. Stabilization of snail by NF-κB is required for inflammation-induced cell migration and invasion. *Cancer Cell* 2009;15: 416–428.
30. Hackett TL, Warner SM, Stefanowicz D, Shaheen F, Pechkovsky DV, Murray LA, Argentieri R, Kicic A, Stick SM, Bai TR, *et al*. Induction of epithelial–mesenchymal transition in primary airway epithelial cells from patients with asthma by transforming growth factor-β1. *Am J Respir Crit Care Med* 2009;180:122–133.
31. Guillot L, Le Goffic R, Bloch S, Escriou N, Akira S, Chignard M, Si-Tahar M. Involvement of Toll-like receptor 3 in the immune response of lung epithelial cells to double-stranded RNA and influenza A virus. *J Biol Chem* 2005;280:5571–5580.
32. Hubner RH, Gitter W, El Mokhtari NE, Mathiak M, Both M, Bolte H, Freitag-Wolf S, Bewig B. Standardized quantification of pulmonary fibrosis in histological samples. *Biotechniques* 2008;44:507–511, 514–517.
33. Moeller A, Ask K, Warburton D, Gauldie J, Kolb M. The bleomycin animal model: a useful tool to investigate treatment options for idiopathic pulmonary fibrosis? *Int J Biochem Cell Biol* 2008;40: 362–382.
34. Evans MJ, Van Winkle LS, Fanucchi MV, Plopper CG. The attenuated fibroblast sheath of the respiratory tract epithelial–mesenchymal trophic unit. *Am J Respir Cell Mol Biol* 1999;21:655–657.
35. Holgate ST. Epithelial damage and response. *Clin Exp Allergy* 2000;30 (suppl 1):37–41.
36. Lambrecht BN, Hammad H. The airway epithelium in asthma. *Nat Med* 2012;18:684–692.
37. Kim KK, Kugler MC, Wolters PJ, Robillard L, Galvez MG, Brumwell AN, Sheppard D, Chapman HA. Alveolar epithelial cell mesenchymal transition develops *in vivo* during pulmonary fibrosis and is regulated by the extracellular matrix. *Proc Natl Acad Sci U S A* 2006;103: 13180–13185.
38. Rock JR, Barkauskas CE, Cronce MJ, Xue Y, Harris JR, Liang J, Noble PW, Hogan BL. Multiple stromal populations contribute to pulmonary fibrosis without evidence for epithelial to mesenchymal transition. *Proc Natl Acad Sci U S A* 2011;108:E1475–E1483.
39. Desai P, Yang J, Tian B, Sun H, Kalita M, Ju H, Paulucci-Holthauzen A, Zhao Y, Brasier AR, Sadygov RG. Mixed-effects model of epithelial–mesenchymal transition reveals rewiring of signaling networks. *Cell Signal* 2015;27:1413–1425.
40. Zhao Y, Tian B, Sadygov RG, Zhang Y, Brasier AR. Integrative proteomic analysis reveals reprograming tumor necrosis factor signaling in epithelial mesenchymal transition. *J Proteomics* 2016; 148:126–138.
41. Aguilera-Aguirre L, Hosoki K, Bacsi A, Radák Z, Sur S, Hegde ML, Tian B, Saavedra-Molina A, Brasier AR, Ba X, *et al*. Whole transcriptome analysis reveals a role for OGG1-initiated DNA repair signaling in airway remodeling. *Free Radic Biol Med* 2015;89:20–33.
42. Choudhary S, Boldogh I, Brasier AR. Inside-out signaling pathways from nuclear reactive oxygen species control pulmonary innate immunity. *J Innate Immun* 2016;8:143–155.
43. Kinnier CV, Martinu T, Gowdy KM, Nugent JL, Kelly FL, Palmer SM. Innate immune activation by the viral PAMP poly I:C potentiates pulmonary graft-versus-host disease after allogeneic hematopoietic cell transplant. *Transpl Immunol* 2011;24:83–93.
44. Vareille M, Kieninger E, Edwards MR, Regamey N. The airway epithelium: soldier in the fight against respiratory viruses. *Clin Microbiol Rev* 2011;24:210–229.
45. Lazo JS, Hoyt DG, Sebti SM, Pitt BR. Bleomycin: a pharmacologic tool in the study of the pathogenesis of interstitial pulmonary fibrosis. *Pharmacol Ther* 1990;47:347–358.
46. Izbicki G, Segel MJ, Christensen TG, Conner MW, Breuer R. Time course of bleomycin-induced lung fibrosis. *Int J Exp Pathol* 2002; 83:111–119.
47. Li XW, Wu YH, Li XH, Li D, Du J, Hu CP, Li YJ. Role of eukaryotic translation initiation factor 3a in bleomycin-induced pulmonary fibrosis. *Eur J Pharmacol* 2015;749:89–97.
48. Reinert T, Serodio da Rocha Baldotto C, Nunes FAP, Alves de Souza Scheliga A. Bleomycin-induced lung injury. *J Cancer Res* 2013;2013: 480608.
49. Johnston NW, Sears MR. Asthma exacerbations. 1: epidemiology. *Thorax* 2006;61:722–728.
50. Wilkinson TM, Donaldson GC, Johnston SL, Openshaw PJ, Wedzicha JA. Respiratory syncytial virus, airway inflammation, and FEV_1 decline in patients with chronic obstructive pulmonary disease. *Am J Respir Crit Care Med* 2006;173:871–876.
51. van Ewijk BE, van der Zalm MM, Wolfs TFW, van der Ent CK. Viral respiratory infections in cystic fibrosis. *J Cyst Fibros* 2005;4:31–36.
52. Donaldson GC, Seemungal TA, Patel IS, Bhowmik A, Wilkinson TM, Hurst JR, Maccallum PK, Wedzicha JA. Airway and systemic inflammation and decline in lung function in patients with COPD. *Chest* 2005;128:1995–2004.
53. Barnes PJ, Celli BR. Systemic manifestations and comorbidities of COPD. *Eur Respir J* 2009;33:1165–1185.